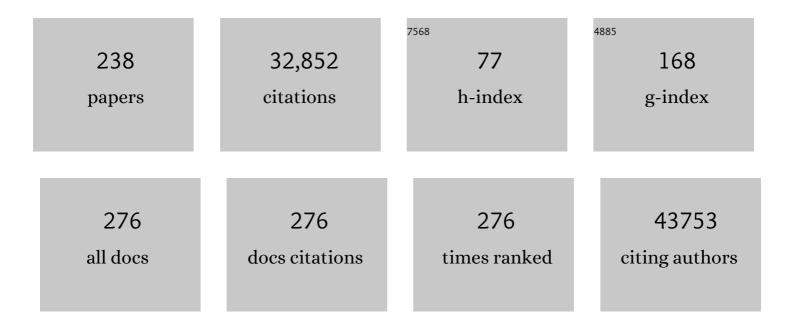


List of Publications by Year in descending order

Source: https://exaly.com/author-pdf/1442269/publications.pdf Version: 2024-02-01



Ηλολλμ

#	Article	IF	CITATIONS
1	R/qtl: QTL mapping in experimental crosses. Bioinformatics, 2003, 19, 889-890.	4.1	3,197
2	Inflammasome-activated gasdermin D causes pyroptosis by forming membrane pores. Nature, 2016, 535, 153-158.	27.8	2,143
3	Brain-Region-Specific Organoids Using Mini-bioreactors for Modeling ZIKV Exposure. Cell, 2016, 165, 1238-1254.	28.9	1,680
4	Unified Polymerization Mechanism for the Assembly of ASC-Dependent Inflammasomes. Cell, 2014, 156, 1193-1206.	28.9	1,035
5	Increased methylation variation in epigenetic domains across cancer types. Nature Genetics, 2011, 43, 768-775.	21.4	968
6	Reversing DNA Methylation: Mechanisms, Genomics, and Biological Functions. Cell, 2014, 156, 45-68.	28.9	914
7	Gasdermin E suppresses tumour growth by activating anti-tumour immunity. Nature, 2020, 579, 415-420.	27.8	900
8	The Pore-Forming Protein Gasdermin D Regulates Interleukin-1 Secretion from Living Macrophages. Immunity, 2018, 48, 35-44.e6.	14.3	789
9	5-hmC–mediated epigenetic dynamics during postnatal neurodevelopment and aging. Nature Neuroscience, 2011, 14, 1607-1616.	14.8	746
10	Pathogen blockade of TAK1 triggers caspase-8–dependent cleavage of gasdermin D and cell death. Science, 2018, 362, 1064-1069.	12.6	639
11	FDA-approved disulfiram inhibits pyroptosis by blocking gasdermin D pore formation. Nature Immunology, 2020, 21, 736-745.	14.5	555
12	Large histone H3 lysine 9 dimethylated chromatin blocks distinguish differentiated from embryonic stem cells. Nature Genetics, 2009, 41, 246-250.	21.4	540
13	Genome-wide Profiling of 5-Formylcytosine Reveals Its Roles in Epigenetic Priming. Cell, 2013, 153, 678-691.	28.9	502
14	Structural mechanism for NEK7-licensed activation of NLRP3 inflammasome. Nature, 2019, 570, 338-343.	27.8	467
15	Genome-wide Analysis Reveals TET- and TDG-Dependent 5-Methylcytosine Oxidation Dynamics. Cell, 2013, 153, 692-706.	28.9	440
16	An endogenous caspase-11 ligand elicits interleukin-1 release from living dendritic cells. Science, 2016, 352, 1232-1236.	12.6	419
17	Long-Lived Plasma Cells Are Contained within the CD19â^'CD38hiCD138+ Subset in Human Bone Marrow. Immunity, 2015, 43, 132-145.	14.3	415
18	A Bayesian hierarchical model to detect differentially methylated loci from single nucleotide resolution sequencing data. Nucleic Acids Research, 2014, 42, e69-e69.	14.5	405

#	Article	IF	CITATIONS
19	Comprehensive high-throughput arrays for relative methylation (CHARM). Genome Research, 2008, 18, 780-790.	5.5	379
20	Epigenomic reprogramming during pancreatic cancer progression links anabolic glucose metabolism to distant metastasis. Nature Genetics, 2017, 49, 367-376.	21.4	365
21	Hydrolysis of 2′3′-cGAMP by ENPP1 and design of nonhydrolyzable analogs. Nature Chemical Biology, 2014, 10, 1043-1048.	8.0	348
22	Cryo-EM structure of the activated NAIP2-NLRC4 inflammasome reveals nucleated polymerization. Science, 2015, 350, 404-409.	12.6	347
23	Genome-scale epigenetic reprogramming during epithelial-to-mesenchymal transition. Nature Structural and Molecular Biology, 2011, 18, 867-874.	8.2	340
24	Differential methylation analysis for BS-seq data under general experimental design. Bioinformatics, 2016, 32, 1446-1453.	4.1	336
25	Channelling inflammation: gasdermins in physiology and disease. Nature Reviews Drug Discovery, 2021, 20, 384-405.	46.4	323
26	Fcl ³ R-mediated SARS-CoV-2 infection of monocytes activates inflammation. Nature, 2022, 606, 576-584.	27.8	314
27	The Structure and Dynamics of Higher-Order Assemblies: Amyloids, Signalosomes, and Granules. Cell, 2016, 165, 1055-1066.	28.9	311
28	Cryo-EM structure of the gasdermin A3 membrane pore. Nature, 2018, 557, 62-67.	27.8	301
29	Gasdermin D pore structure reveals preferential release of mature interleukin-1. Nature, 2021, 593, 607-611.	27.8	298
30	Kdm2b maintains murine embryonic stem cell status by recruiting PRC1 complex to CpG islands of developmental genes. Nature Cell Biology, 2013, 15, 373-384.	10.3	292
31	Epitranscriptomic m6A Regulation of Axon Regeneration in the Adult Mammalian Nervous System. Neuron, 2018, 97, 313-325.e6.	8.1	292
32	Higher-Order Assemblies in a New Paradigm of Signal Transduction. Cell, 2013, 153, 287-292.	28.9	291
33	U1 small nuclear ribonucleoprotein complex and RNA splicing alterations in Alzheimer's disease. Proceedings of the National Academy of Sciences of the United States of America, 2013, 110, 16562-16567.	7.1	268
34	The ubiquitin-modifying enzyme A20 restricts ubiquitination of the kinase RIPK3 and protects cells from necroptosis. Nature Immunology, 2015, 16, 618-627.	14.5	224
35	A Specific LSD1/KDM1A Isoform Regulates Neuronal Differentiation through H3K9 Demethylation. Molecular Cell, 2015, 57, 957-970.	9.7	221
36	Active Pin1 is a key target of all-trans retinoic acid in acute promyelocytic leukemia and breast cancer. Nature Medicine, 2015, 21, 457-466.	30.7	220

#	Article	IF	CITATIONS
37	HDAC6 mediates an aggresome-like mechanism for NLRP3 and pyrin inflammasome activation. Science, 2020, 369, .	12.6	218
38	The Structure of the Necrosome RIPK1-RIPK3 Core, a Human Hetero-Amyloid Signaling Complex. Cell, 2018, 173, 1244-1253.e10.	28.9	216
39	An Acetylation Switch of the NLRP3 Inflammasome Regulates Aging-Associated Chronic Inflammation and Insulin Resistance. Cell Metabolism, 2020, 31, 580-591.e5.	16.2	213
40	A new shrinkage estimator for dispersion improves differential expression detection in RNA-seq data. Biostatistics, 2013, 14, 232-243.	1.5	210
41	Inflammasome activation at the crux of severe COVID-19. Nature Reviews Immunology, 2021, 21, 694-703.	22.7	210
42	Detection of differentially methylated regions from whole-genome bisulfite sequencing data without replicates. Nucleic Acids Research, 2015, 43, gkv715.	14.5	203
43	Reactivation of PTEN tumor suppressor for cancer treatment through inhibition of a MYC-WWP1 inhibitiory pathway. Science, 2019, 364, .	12.6	194
44	DNA N6-methyladenine is dynamically regulated in the mouse brain following environmental stress. Nature Communications, 2017, 8, 1122.	12.8	182
45	Inhibition of ileal bile acid uptake protects against nonalcoholic fatty liver disease in high-fat diet–fed mice. Science Translational Medicine, 2016, 8, 357ra122.	12.4	160
46	Genome-wide DNA hydroxymethylation changes are associated with neurodevelopmental genes in the developing human cerebellum. Human Molecular Genetics, 2012, 21, 5500-5510.	2.9	157
47	Molecular signatures associated with ZIKV exposure in human cortical neural progenitors. Nucleic Acids Research, 2016, 44, 8610-8620.	14.5	155
48	Molecular Mechanism of V(D)J Recombination from Synaptic RAG1-RAG2 Complex Structures. Cell, 2015, 163, 1138-1152.	28.9	154
49	Redefining CpG islands using hidden Markov models. Biostatistics, 2010, 11, 499-514.	1.5	151
50	Inhibition of histone lysine-specific demethylase 1 elicits breast tumor immunity and enhances antitumor efficacy of immune checkpoint blockade. Oncogene, 2019, 38, 390-405.	5.9	149
51	Ruxolitinib reverses dysregulated T helper cell responses and controls autoimmunity caused by a novel signal transducer and activator of transcription 1 (STAT1) gain-of-function mutation. Journal of Allergy and Clinical Immunology, 2017, 139, 1629-1640.e2.	2.9	147
52	A single domain antibody fragment that recognizes the adaptor ASC defines the role of ASC domains in inflammasome assembly. Journal of Experimental Medicine, 2016, 213, 771-790.	8.5	145
53	Single-base resolution analysis of active DNA demethylation using methylase-assisted bisulfite sequencing. Nature Biotechnology, 2014, 32, 1231-1240.	17.5	139
54	AID Recognizes Structured DNA for Class Switch Recombination. Molecular Cell, 2017, 67, 361-373.e4.	9.7	136

#	Article	IF	CITATIONS
55	Molecular basis of caspase-1 polymerization and its inhibition by a new capping mechanism. Nature Structural and Molecular Biology, 2016, 23, 416-425.	8.2	135
56	Structural Basis and Functional Role of Intramembrane Trimerization of the Fas/CD95 Death Receptor. Molecular Cell, 2016, 61, 602-613.	9.7	135
57	Cell-Cycle Control of Developmentally Regulated Transcription Factors Accounts for Heterogeneity in Human Pluripotent Cells. Stem Cell Reports, 2013, 1, 532-544.	4.8	129
58	Structures and gating mechanism of human TRPM2. Science, 2018, 362, .	12.6	129
59	Fragile X mental retardation protein modulates the stability of its m6A-marked messenger RNA targets. Human Molecular Genetics, 2018, 27, 3936-3950.	2.9	129
60	Cryo-EM Structure of Caspase-8 Tandem DED Filament Reveals Assembly and Regulation Mechanisms of the Death-Inducing Signaling Complex. Molecular Cell, 2016, 64, 236-250.	9.7	128
61	NLRP3 cages revealed by full-length mouse NLRP3 structure control pathway activation. Cell, 2021, 184, 6299-6312.e22.	28.9	120
62	Gasdermin D activity in inflammation and host defense. Science Immunology, 2019, 4, .	11.9	119
63	R/qtlbim: QTL with Bayesian Interval Mapping in experimental crosses. Bioinformatics, 2007, 23, 641-643.	4.1	115
64	DPP9 sequesters the CÂterminus of NLRP1 to repress inflammasome activation. Nature, 2021, 592, 778-783.	27.8	114
65	Estimating and accounting for tumor purity in the analysis of DNA methylation data from cancer studies. Genome Biology, 2017, 18, 17.	8.8	112
66	IRAK4 Dimerization and trans -Autophosphorylation Are Induced by Myddosome Assembly. Molecular Cell, 2014, 55, 891-903.	9.7	108
67	Higher-Order Clustering of the Transmembrane Anchor of DR5 Drives Signaling. Cell, 2019, 176, 1477-1489.e14.	28.9	104
68	Sirolimus for the treatment of progressive kaposiform hemangioendothelioma: A multicenter retrospective study. International Journal of Cancer, 2017, 141, 848-855.	5.1	103
69	Cryo-EM structures of ASC and NLRC4 CARD filaments reveal a unified mechanism of nucleation and activation of caspase-1. Proceedings of the National Academy of Sciences of the United States of America, 2018, 115, 10845-10852.	7.1	103
70	Ubiquitin-Mediated Regulation of RIPK1 Kinase Activity Independent of IKK and MK2. Molecular Cell, 2018, 69, 566-580.e5.	9.7	102
71	HMMR Maintains the Stemness and Tumorigenicity of Glioblastoma Stem-like Cells. Cancer Research, 2014, 74, 3168-3179.	0.9	101
72	NanoStringDiff: a novel statistical method for differential expression analysis based on NanoString nCounter data. Nucleic Acids Research, 2016, 44, gkw677.	14.5	100

#	Article	IF	CITATIONS
73	Mechanism and Regulation of Gasdermin-Mediated Cell Death. Cold Spring Harbor Perspectives in Biology, 2020, 12, a036400.	5.5	100
74	Phase separation drives RNA virus-induced activation of the NLRP6 inflammasome. Cell, 2021, 184, 5759-5774.e20.	28.9	97
75	The nuclear matrix protein HNRNPU maintains 3D genome architecture globally in mouse hepatocytes. Genome Research, 2018, 28, 192-202.	5.5	91
76	Structure of cytoplasmic ring of nuclear pore complex by integrative cryo-EM and AlphaFold. Science, 2022, 376, .	12.6	89
77	Characterization of T and B cell repertoire diversity in patients with RAG deficiency. Science Immunology, 2016, 1, .	11.9	88
78	Structures of a Complete Human V-ATPase Reveal Mechanisms of Its Assembly. Molecular Cell, 2020, 80, 501-511.e3.	9.7	88
79	Subtelomeric hotspots of aberrant 5-hydroxymethylcytosine-mediated epigenetic modifications during reprogramming to pluripotency. Nature Cell Biology, 2013, 15, 700-711.	10.3	87
80	Assembly mechanism of the CARMA1–BCL10–MALT1–TRAF6 signalosome. Proceedings of the National Academy of Sciences of the United States of America, 2018, 115, 1499-1504.	7.1	87
81	SERPINB1-mediated checkpoint of inflammatory caspase activation. Nature Immunology, 2019, 20, 276-287.	14.5	87
82	Molecular mechanism for NLRP6 inflammasome assembly and activation. Proceedings of the National Academy of Sciences of the United States of America, 2019, 116, 2052-2057.	7.1	86
83	Zika virus directly infects peripheral neurons and induces cell death. Nature Neuroscience, 2017, 20, 1209-1212.	14.8	85
84	METTL4 is an snRNA m6Am methyltransferase that regulates RNA splicing. Cell Research, 2020, 30, 544-547.	12.0	84
85	Plasticity in PYD assembly revealed by cryo-EM structure of the PYD filament of AIM2. Cell Discovery, 2015, 1, .	6.7	83
86	A genomeâ€wide profiling of brain DNA hydroxymethylation in Alzheimer's disease. Alzheimer's and Dementia, 2017, 13, 674-688.	0.8	83
87	Role of endoplasmic reticulum stress signalling in diabetic endothelial dysfunction and atherosclerosis. Diabetes and Vascular Disease Research, 2017, 14, 14-23.	2.0	83
88	Ten-eleven translocation 2 interacts with forkhead box O3 and regulates adult neurogenesis. Nature Communications, 2017, 8, 15903.	12.8	82
89	PROPER: comprehensive power evaluation for differential expression using RNA-seq. Bioinformatics, 2015, 31, 233-241.	4.1	80
90	NLRP3 Inflammasome Assembly in Neutrophils Is Supported by PAD4 and Promotes NETosis Under Sterile Conditions. Frontiers in Immunology, 2021, 12, 683803.	4.8	79

#	Article	IF	CITATIONS
91	Fragile X premutation RNA is sufficient to cause primary ovarian insufficiency in mice. Human Molecular Genetics, 2012, 21, 5039-5047.	2.9	78
92	Lin28A Binds Active Promoters and Recruits Tet1 to Regulate Gene Expression. Molecular Cell, 2016, 61, 153-160.	9.7	74
93	Cryo-EM structure of the DNA-PK holoenzyme. Proceedings of the National Academy of Sciences of the United States of America, 2017, 114, 7367-7372.	7.1	74
94	Active N6-Methyladenine Demethylation by DMAD Regulates Gene Expression by Coordinating with Polycomb Protein in Neurons. Molecular Cell, 2018, 71, 848-857.e6.	9.7	71
95	Cryo-EM structure of an activated GPCR–G protein complex in lipid nanodiscs. Nature Structural and Molecular Biology, 2021, 28, 258-267.	8.2	71
96	Dedicator of cytokinesis 8 regulates signal transducer and activator of transcription 3 activation and promotes TH17Âcell differentiation. Journal of Allergy and Clinical Immunology, 2016, 138, 1384-1394.e2.	2.9	70
97	The Inflammasome Adaptor ASC Induces Procaspase-8 Death Effector Domain Filaments. Journal of Biological Chemistry, 2015, 290, 29217-29230.	3.4	69
98	Peptidoglycan-Sensing Receptors Trigger the Formation of Functional Amyloids of the Adaptor Protein Imd to Initiate Drosophila NF-I®B Signaling. Immunity, 2017, 47, 635-647.e6.	14.3	63
99	Modeling Parkinson's disease in monkeys for translational studies, a critical analysis. Experimental Neurology, 2014, 256, 133-143.	4.1	62
100	Crystal structure of the WD40 domain dimer of LRRK2. Proceedings of the National Academy of Sciences of the United States of America, 2019, 116, 1579-1584.	7.1	60
101	Crystal structure of human IRAK1. Proceedings of the National Academy of Sciences of the United States of America, 2017, 114, 13507-13512.	7.1	59
102	The hierarchical structural architecture of inflammasomes, supramolecular inflammatory machines. Current Opinion in Structural Biology, 2015, 31, 75-83.	5.7	58
103	Targeting stem-loop 1 of the SARS-CoV-2 5â€ ² UTR to suppress viral translation and Nsp1 evasion. Proceedings of the National Academy of Sciences of the United States of America, 2022, 119, .	7.1	56
104	Eating the Dead to Keep Atherosclerosis at Bay. Frontiers in Cardiovascular Medicine, 2017, 4, 2.	2.4	54
105	HDAC5–LSD1 axis regulates antineoplastic effect of natural HDAC inhibitor sulforaphane in human breast cancer cells. International Journal of Cancer, 2018, 143, 1388-1401.	5.1	54
106	TRPM2, linking oxidative stress and Ca2+ permeation to NLRP3 inflammasome activation. Current Opinion in Immunology, 2020, 62, 131-135.	5.5	54
107	Multiple domain interfaces mediate SARM1 autoinhibition. Proceedings of the National Academy of Sciences of the United States of America, 2021, 118, .	7.1	54
108	Structure of a microtubule-bound axonemal dynein. Nature Communications, 2021, 12, 477.	12.8	54

#	Article	IF	CITATIONS
109	Ectopic lipid accumulation: potential role in tubular injury and inflammation in diabetic kidney disease. Clinical Science, 2018, 132, 2407-2422.	4.3	53
110	A species-generalized probabilistic model-based definition of CpG islands. Mammalian Genome, 2009, 20, 674-80.	2.2	52
111	Genome-wide alteration of 5-hydroxymethylcytosine in a mouse model of fragile X-associated tremor/ataxia syndrome. Human Molecular Genetics, 2014, 23, 1095-1107.	2.9	52
112	Epsin deficiency promotes lymphangiogenesis through regulation of VEGFR3 degradation in diabetes. Journal of Clinical Investigation, 2018, 128, 4025-4043.	8.2	52
113	Crystal Structure of the F27G AIM2 PYD Mutant and Similarities of Its Self-Association to DED/DED Interactions. Journal of Molecular Biology, 2014, 426, 1420-1427.	4.2	51
114	Specific covalent inhibition of MALT1 paracaspase suppresses B cell lymphoma growth. Journal of Clinical Investigation, 2018, 128, 4397-4412.	8.2	51
115	Predicting tumor purity from methylation microarray data. Bioinformatics, 2015, 31, 3401-3405.	4.1	50
116	A novel statistical method for quantitative comparison of multiple ChIP-seq datasets. Bioinformatics, 2015, 31, 1889-1896.	4.1	48
117	Integrating Next-Generation Genomic Sequencing and Mass Spectrometry To Estimate Allele-Specific Protein Abundance in Human Brain. Journal of Proteome Research, 2017, 16, 3336-3347.	3.7	48
118	InfiniumPurify: An R package for estimating and accounting for tumor purity in cancer methylation research. Genes and Diseases, 2018, 5, 43-45.	3.4	48
119	Mechanism of filament formation in UPA-promoted CARD8 and NLRP1 inflammasomes. Nature Communications, 2021, 12, 189.	12.8	48
120	Dipeptidyl peptidase 9 sets a threshold for CARD8 inflammasome formation by sequestering its active C-terminal fragment. Immunity, 2021, 54, 1392-1404.e10.	14.3	47
121	Base-resolution methylation patterns accurately predict transcription factor bindings in vivo. Nucleic Acids Research, 2015, 43, 2757-2766.	14.5	46
122	Ten-Eleven Translocation Proteins Modulate the Response to Environmental Stress in Mice. Cell Reports, 2018, 25, 3194-3203.e4.	6.4	46
123	MacroH2A1 associates with nuclear lamina and maintains chromatin architecture in mouse liver cells. Scientific Reports, 2015, 5, 17186.	3.3	44
124	Mind Bomb Regulates Cell Death during TNF Signaling by Suppressing RIPK1's Cytotoxic Potential. Cell Reports, 2018, 23, 470-484.	6.4	42
125	TOAST: improving reference-free cell composition estimation by cross-cell type differential analysis. Genome Biology, 2019, 20, 190.	8.8	42
126	Myeloid-Specific Deletion of Epsins 1 and 2 Reduces Atherosclerosis by Preventing LRP-1 Downregulation. Circulation Research, 2019, 124, e6-e19.	4.5	41

#	Article	IF	CITATIONS
127	Euchromatin islands in large heterochromatin domains are enriched for CTCF binding and differentially DNA-methylated regions. BMC Genomics, 2012, 13, 566.	2.8	40
128	Mapping the Broad Structural and Mechanical Properties of Amyloid Fibrils. Biophysical Journal, 2017, 112, 584-594.	0.5	40
129	DNA melting initiates the RAG catalytic pathway. Nature Structural and Molecular Biology, 2018, 25, 732-742.	8.2	40
130	Selective Targeting of a Novel Epsin–VEGFR2 Interaction Promotes VEGF-Mediated Angiogenesis. Circulation Research, 2016, 118, 957-969.	4.5	35
131	Dissecting differential signals in high-throughput data from complex tissues. Bioinformatics, 2019, 35, 3898-3905.	4.1	35
132	Disease prediction by cell-free DNA methylation. Briefings in Bioinformatics, 2019, 20, 585-597.	6.5	35
133	CG14906 (mettl4) mediates m6A methylation of U2 snRNA in Drosophila. Cell Discovery, 2020, 6, 44.	6.7	35
134	Structures and functions of the inflammasome engine. Journal of Allergy and Clinical Immunology, 2021, 147, 2021-2029.	2.9	35
135	Two-phase differential expression analysis for single cell RNA-seq. Bioinformatics, 2018, 34, 3340-3348.	4.1	34
136	Mechanism of ubiquitin transfer promoted by TRAF6. Proceedings of the National Academy of Sciences of the United States of America, 2018, 115, 1783-1788.	7.1	34
137	Functional characterization of lysine-specific demethylase 2 (LSD2/KDM1B) in breast cancer progression. Oncotarget, 2017, 8, 81737-81753.	1.8	34
138	BTK operates a phospho-tyrosine switch to regulate NLRP3 inflammasome activity. Journal of Experimental Medicine, 2021, 218, .	8.5	33
139	TRIM21 regulates pyroptotic cell death by promoting Gasdermin D oligomerization. Cell Death and Differentiation, 2022, 29, 439-450.	11.2	33
140	Reply to "Reassessing the abundance of H3K9me2 chromatin domains in embryonic stem cells― Nature Genetics, 2010, 42, 5-6.	21.4	32
141	Accounting for tumor purity improves cancer subtype classification from DNA methylation data. Bioinformatics, 2017, 33, 2651-2657.	4.1	32
142	Homogeneous Oligomers of Pro-apoptotic BAX Reveal Structural Determinants of Mitochondrial Membrane Permeabilization. Molecular Cell, 2020, 79, 68-83.e7.	9.7	32
143	Disulfiram use is associated with lower risk of COVID-19: A retrospective cohort study. PLoS ONE, 2021, 16, e0259061.	2.5	32
144	Intensity normalization improves color calling in SOLiD sequencing. Nature Methods, 2010, 7, 336-337.	19.0	31

#	Article	IF	CITATIONS
145	Deletion of Atbf1/Zfhx3 In Mouse Prostate Causes Neoplastic Lesions, Likely by Attenuation of Membrane and Secretory Proteins and Multiple Signaling Pathways. Neoplasia, 2014, 16, 377-389.	5.3	31
146	Plasmodium knowlesi gene expression differs in ex vivo compared to in vitro blood-stage cultures. Malaria Journal, 2015, 14, 110.	2.3	31
147	Accurate feature selection improves single-cell RNA-seq cell clustering. Briefings in Bioinformatics, 2021, 22, .	6.5	31
148	Base-resolution profiling of active DNA demethylation using MAB-seq and caMAB-seq. Nature Protocols, 2016, 11, 1081-1100.	12.0	30
149	Modulation of virus-induced NF-l̂®B signaling by NEMO coiled coil mimics. Nature Communications, 2020, 11, 1786.	12.8	30
150	Could AlphaFold revolutionize chemical therapeutics?. Nature Structural and Molecular Biology, 2021, 28, 771-772.	8.2	30
151	Overlapping euchromatin/heterochromatin- associated marks are enriched in imprinted gene regions and predict allele-specific modification. Genome Research, 2008, 18, 1806-1813.	5.5	29
152	5-Hydroxymethylcytosine alterations in the human postmortem brains of autism spectrum disorder. Human Molecular Genetics, 2018, 27, 2955-2964.	2.9	28
153	Combined immunodeficiency caused by a loss-of-function mutation in DNA polymerase delta 1. Journal of Allergy and Clinical Immunology, 2020, 145, 391-401.e8.	2.9	28
154	LIN28 coordinately promotes nucleolar/ribosomal functions and represses the 2C-like transcriptional program in pluripotent stem cells. Protein and Cell, 2022, 13, 490-512.	11.0	28
155	Evidence for M1-Linked Polyubiquitin-Mediated Conformational Change in NEMO. Journal of Molecular Biology, 2017, 429, 3793-3800.	4.2	27
156	Local false discovery rate estimation using feature reliability in LC/MS metabolomics data. Scientific Reports, 2015, 5, 17221.	3.3	24
157	Epsin-mediated degradation of IP3R1 fuels atherosclerosis. Nature Communications, 2020, 11, 3984.	12.8	24
158	Higher-order assemblies in innate immune and inflammatory signaling: A general principle in cell biology. Current Opinion in Cell Biology, 2020, 63, 194-203.	5.4	24
159	SPARCLE, a p53-induced lncRNA, controls apoptosis after genotoxic stress by promoting PARP-1 cleavage. Molecular Cell, 2022, 82, 785-802.e10.	9.7	24
160	CIDE domains form functionally important higher-order assemblies for DNA fragmentation. Proceedings of the National Academy of Sciences of the United States of America, 2017, 114, 7361-7366.	7.1	23
161	Structural and mechanistic elucidation of inflammasome signaling by cryo-EM. Current Opinion in Structural Biology, 2019, 58, 18-25.	5.7	23
162	Instant Hydrogelation Inspired by Inflammasomes. Angewandte Chemie - International Edition, 2017, 56, 7579-7583.	13.8	22

#	Article	IF	CITATIONS
163	Keeping the Death Protein in Check. Immunity, 2019, 51, 1-2.	14.3	22
164	Non-alcoholic Steatohepatitis Pathogenesis, Diagnosis, and Treatment. Frontiers in Cardiovascular Medicine, 2021, 8, 742382.	2.4	22
165	A comprehensive comparison of supervised and unsupervised methods for cell type identification in single-cell RNA-seq. Briefings in Bioinformatics, 2022, 23, .	6.5	22
166	pH regulates potassium conductance and drives a constitutive proton current in human TMEM175. Science Advances, 2022, 8, eabm1568.	10.3	22
167	Differential methylation analysis for bisulfite sequencing using DSS. Quantitative Biology, 2019, 7, 327-334.	O.5	21
168	Evaluation of some aspects in supervised cell type identification for single-cell RNA-seq: classifier, feature selection, and reference construction. Genome Biology, 2021, 22, 264.	8.8	21
169	Structural gymnastics of RAG-mediated DNA cleavage in V(D)J recombination. Current Opinion in Structural Biology, 2018, 53, 178-186.	5.7	20
170	Monitoring gasdermin pore formation in vitro. Methods in Enzymology, 2019, 625, 95-107.	1.0	20
171	Epsins 1 and 2 promote NEMO linear ubiquitination via LUBAC to drive breast cancer development. Journal of Clinical Investigation, 2021, 131, .	8.2	18
172	INAVA-ARNO complexes bridge mucosal barrier function with inflammatory signaling. ELife, 2018, 7, .	6.0	17
173	The Role of Endothelial-to-Mesenchymal Transition in Cardiovascular Disease. Cells, 2022, 11, 1834.	4.1	16
174	Peptide-based covalent inhibitors of MALT1 paracaspase. Bioorganic and Medicinal Chemistry Letters, 2019, 29, 1336-1339.	2.2	15
175	A nanobody targeting the LIN28:let-7 interaction fragment of TUT4 blocks uridylation of let-7. Proceedings of the National Academy of Sciences of the United States of America, 2020, 117, 4653-4663.	7.1	15
176	The CBM signalosome: Potential therapeutic target for aggressive lymphoma?. Cytokine and Growth Factor Reviews, 2014, 25, 175-183.	7.2	14
177	Supramolecular organizing centers (SMOCs) as signaling machines in innate immune activation. Science China Life Sciences, 2015, 58, 1067-1072.	4.9	14
178	Conformational flexibility and inhibitor binding to unphosphorylated interleukin-1 receptor–associated kinase 4 (IRAK4). Journal of Biological Chemistry, 2019, 294, 4511-4519.	3.4	14
179	Quinoline and thiazolopyridine allosteric inhibitors of MALT1. Bioorganic and Medicinal Chemistry Letters, 2019, 29, 1694-1698.	2.2	14
180	PolyaPeak: Detecting Transcription Factor Binding Sites from ChIP-seq Using Peak Shape Information. PLoS ONE, 2014, 9, e89694.	2.5	13

#	Article	IF	CITATIONS
181	Tumor purity and differential methylation in cancer epigenomics. Briefings in Functional Genomics, 2016, 15, elw016.	2.7	13
182	Experimental Design and Power Calculation for RNA-seq Experiments. Methods in Molecular Biology, 2016, 1418, 379-390.	0.9	13
183	ROC Curve Analysis in the Presence of Imperfect Reference Standards. Statistics in Biosciences, 2017, 9, 91-104.	1.2	13
184	Fibrinogenâ€like proteinâ€2 causes deterioration in cardiac function in experimental autoimmune myocarditis rats through regulation of programmed deathâ€1 and inflammatory cytokines. Immunology, 2018, 153, 246-252.	4.4	13
185	Electrostatic influence on IL-1 transport through the GSDMD pore. Proceedings of the National Academy of Sciences of the United States of America, 2022, 119, .	7.1	13
186	JAMIE: joint analysis of multiple ChIP-chip experiments. Bioinformatics, 2010, 26, 1864-1870.	4.1	12
187	Endothelial epsins as regulators and potential therapeutic targets of tumor angiogenesis. Cellular and Molecular Life Sciences, 2017, 74, 393-398.	5.4	12
188	A comprehensive review of computational prediction of genome-wide features. Briefings in Bioinformatics, 2020, 21, 120-134.	6.5	12
189	Mechanism of TRPM 2 channel gating revealed by cryo―EM. FEBS Journal, 2019, 286, 3333-3339.	4.7	12
190	Inflammasome Activation and Pyroptosis via a Lipid-regulated SIRT1-p53-ASC Axis in Macrophages From Male Mice and Humans. Endocrinology, 2022, 163, .	2.8	12
191	A High Throughput Whole Blood Assay for Analysis of Multiple Antigen-Specific T Cell Responses in Human <i>Mycobacterium tuberculosis</i> Infection. Journal of Immunology, 2018, 200, 3008-3019.	0.8	11
192	Ethnicity-specific and overlapping alterations of brain hydroxymethylome in Alzheimer's disease. Human Molecular Genetics, 2020, 29, 149-158.	2.9	11
193	Discovery of a Selective, Covalent IRAK1 Inhibitor with Antiproliferative Activity in MYD88 Mutated B-Cell Lymphoma. ACS Medicinal Chemistry Letters, 2020, 11, 2238-2243.	2.8	11
194	Epsins in vascular development, function and disease. Cellular and Molecular Life Sciences, 2021, 78, 833-842.	5.4	11
195	Disulfide Bond Formation and N-Glycosylation Modulate Protein-Protein Interactions in GPI-Transamidase (GPIT). Scientific Reports, 2017, 7, 45912.	3.3	10
196	Detecting m6A methylation regions from Methylated RNA Immunoprecipitation Sequencing. Bioinformatics, 2021, 37, 2818-2824.	4.1	10
197	Statistical Challenges in Analyzing Methylation and Long-Range Chromosomal Interaction Data. Statistics in Biosciences, 2016, 8, 284-309.	1.2	9
198	Understanding CARD Tricks in Apoptosomes. Structure, 2017, 25, 575-577.	3.3	8

#	Article	IF	CITATIONS
199	Age-related DNA hydroxymethylation is enriched for gene expression and immune system processes in human peripheral blood. Epigenetics, 2020, 15, 294-306.	2.7	8
200	Mimetic peptide of ubiquitin-interacting motif of epsin as a cancer therapeutic-perspective in brain tumor therapy through regulating VEGFR2 signaling. Vessel Plus, 2017, 1, 3-11.	0.4	8
201	Ragulator-Rag and ROS TORment gasdermin D pore formation. Trends in Immunology, 2021, 42, 948-950.	6.8	8
202	Nonmetastatic breast cancer patients subsequently developing second primary malignancy: A populationâ€based study. Cancer Medicine, 2021, 10, 8662-8672.	2.8	8
203	PLEMT: A Novel Pseudolikelihood-Based EM Test for Homogeneity in Generalized Exponential Tilt Mixture Models. Journal of the American Statistical Association, 2017, 112, 1393-1404.	3.1	7
204	Instant Hydrogelation Inspired by Inflammasomes. Angewandte Chemie, 2017, 129, 7687-7691.	2.0	7
205	Differential gene network analysis from single cell RNA-seq. Journal of Genetics and Genomics, 2017, 44, 331-334.	3.9	7
206	FGL2 knockdown improves heart function through regulation of TLR9 signaling in the experimental autoimmune myocarditis rats. Immunologic Research, 2018, 66, 52-58.	2.9	7
207	Mimicry by a viral <scp>RHIM</scp> . EMBO Reports, 2019, 20, .	4.5	7
208	Gain-of-function mutations in CARD11 promote enhanced aggregation and idiosyncratic signalosome assembly. Cellular Immunology, 2020, 353, 104129.	3.0	7
209	RIP1/RIP3/MLKL Mediates Myocardial Function Through Necroptosis in Experimental Autoimmune Myocarditis. Frontiers in Cardiovascular Medicine, 2021, 8, 696362.	2.4	7
210	CDKL3 promotes osteosarcoma progression by activating Akt/PKB. Life Science Alliance, 2020, 3, e202000648.	2.8	7
211	Diabetes and Its Cardiovascular Complications: Comprehensive Network and Systematic Analyses. Frontiers in Cardiovascular Medicine, 2022, 9, 841928.	2.4	7
212	KDM1A Identified as a Potential Oncogenic Driver and Prognostic Biomarker via Multi-Omics Analysis. Canadian Journal of Infectious Diseases and Medical Microbiology, 2021, 2021, 1-18.	1.9	5
213	Bad germs are trapped. Cell Research, 2018, 28, 141-142.	12.0	4
214	Downregulation of <i>TOP2</i> modulates neurodegeneration caused by GGGGCC expanded repeats. Human Molecular Genetics, 2021, 30, 893-901.	2.9	4
215	BCL10 Gain-of-Function Mutations Aberrantly Induce Canonical and Non-Canonical NF-Kb Activation and Resistance to Ibrutinib in ABC-DLBCL. Blood, 2020, 136, 2-3.	1.4	4
216	EDClust: an EM–MM hybrid method for cell clustering in multiple-subject single-cell RNA sequencing. Bioinformatics, 2022, 38, 2692-2699.	4.1	4

#	Article	IF	CITATIONS
217	Promiscuity Is Not Always Bad. Molecular Cell, 2014, 54, 208-209.	9.7	3
218	Michael G. Rossmann (1930–2019). Nature Structural and Molecular Biology, 2019, 26, 660-662.	8.2	3
219	STING condensates on ER limit IFN response. Nature Cell Biology, 2021, 23, 299-300.	10.3	3
220	Exploring the Cooccurrence Patterns of Multiple Sets of Genomic Intervals. BioMed Research International, 2013, 2013, 1-7.	1.9	2
221	Measuring the spatial correlations of protein binding sites. Bioinformatics, 2016, 32, 1766-1772.	4.1	2
222	Inflammation NODs to Antagonists of RIP2-XIAP Interaction. Molecular Cell, 2018, 69, 535-536.	9.7	2
223	Purification and cryoelectron microscopy structure determination of human V-ATPase. STAR Protocols, 2021, 2, 100350.	1.2	2
224	Advances toward structure-based drug discovery for inflammasome targets. Journal of Experimental Medicine, 2022, 219, .	8.5	2
225	<i>BCL10</i> Mutations Define Distinct Dependencies Guiding Precision Therapy for DLBCL. Cancer Discovery, 0, , OF1-OF20.	9.4	2
226	FDA-approved disulfiram inhibits pyroptosis by blocking gasdermin D pore formation. , 0, .		1
227	JAMIE: A Software Tool for Jointly Analyzing Multiple ChIP-chip Experiments. Methods in Molecular Biology, 2012, 802, 363-375.	0.9	1
228	Insights into gasdermin pore formation from the structure of a preâ€pore. FASEB Journal, 2019, 33, 779.49.	0.5	1
229	Enhanced Lymphangiogenesis and Lymphatic Function Protects Dietâ€induced Obesity and Insulin Resistance. FASEB Journal, 2019, 33, 662.25.	0.5	1
230	Statistics for Next Generation Sequencing – Meeting Report. Frontiers in Genetics, 2012, 3, 128.	2.3	0
231	Incorporating feature reliability in false discovery rateestimation improves statistical power to detect differentially expressed features. , 2014, , .		0
232	Computer Simulation, Bioinformatics, and Statistical Analysis of Cancer Data and Processes. Cancer Informatics, 2015, 14s2, CIN.S32525.	1.9	0
233	Gene expression profiles of rat MMECs with different glucose levels and <i>fgl2</i> gene silencing. Diabetes/Metabolism Research and Reviews, 2018, 34, e3058.	4.0	0
234	Michael G. Rossmann (1930–2019), pioneer in macromolecular and virus crystallography: scientist, mentor and friend. Acta Crystallographica Section D: Structural Biology, 2019, 75, 523-527.	2.3	0

#	Article	IF	CITATIONS
235	Structural Basis for NLRP6 Inflammasome Assembly and Activation. FASEB Journal, 2019, 33, 779.38.	0.5	0
236	Higherâ€Order Clustering of the Transmembrane Anchor of DR5 Drives Signaling. FASEB Journal, 2019, 33, 792.3.	0.5	0
237	Structures and gating mechanism of human TRPM2. FASEB Journal, 2019, 33, .	0.5	0
238	Expression Signatures of Long Noncoding RNAs in Left Ventricular Noncompaction. Frontiers in Cardiovascular Medicine, 2021, 8, 763858.	2.4	0